Suliman *et al. EURASIP Journal on Wireless Communications and Networking* (2015) 2015:244
DOI 10.1186/s13638-015-0474-3

EURASIP Journal on Wireless Communications and Networking
a SpringerOpen Journal

RESEARCH Open Access

On the effect of false alarm rate on the performance of cognitive radio networks

Isameldin M. Suliman[1*], Janne Lehtomäki[2] and Kenta Umebayashi[3]

Abstract

Spectrum sensing plays a significant role in enabling utilization of spectrum holes by unlicensed secondary users (SUs) in cognitive radio networks (CRNs). Most of the related work concerning spectrum sensing has focused on sensing carried out by incoming secondary users (SUs) aiming at locating spectrum opportunities. However, in order to appropriately protect returning licensed primary users (PUs), SUs should continuously perform spectrum sensing during their ongoing transmissions. An important issue associated with the continuous sensing is the false alarm rate (FAR), which is defined as the average number of false alarms per unit of time and can be modeled by a Poisson process with Poisson parameter λ_{FAR}. In this paper, we address this issue and develop a continuous time Markov chain (CTMC)-based analytical model to evaluate the effect of the false alarm rate on the performance of CRNs. A major feature of the proposed analytical framework is that it takes into account the effects of sensing errors by both incoming SUs looking for free channels to transmit on and the already transmitting SUs expecting the presence of returning PUs. The analytical model also examines the interference tolerance among PUs and SUs as well as the impact of SUs residual self-interference. The performance results show that high λ_{FAR} can severely degrade PUs performance and reduce the overall system resource utilization. However, with increasing PU interference tolerance, PUs performance improves as well. SU residual interference was found to decrease the detection probability resulting in a low PU performance. Extensive simulations validate the analytical model, demonstrating excellent agreement with the theoretical results.

Keywords: Cognitive radio network, Opportunistic spectrum access, False alarm rate, Markov chain, Spectrum sensing, Performance analysis

1 Introduction

With today's inefficient utilization of the scarce radio spectrum, cognitive radio (CR) [1–3] is becoming an important tool for solving the problem of spectrum underutilization. As a result, there has been considerable research effort focusing on CR techniques that enable using radio spectrum efficiently. In CR networks (CRNs), unlicensed secondary users (SUs) employ spectrum sensing [4–6] to discover spectrum holes during the absence of licensed primary users (PUs) before attempting network access. Energy detection [7–9] is the simplest method for detecting the presence of PUs. It is based on calculating the energy of the received samples which is compared to a threshold. If the threshold is exceeded, it is decided that a signal or signals are present. If the sensed channel is free, SUs may be allowed to transmit on that channel.

No matter which detection scheme is used for protecting returning PUs, it will lead to the occurrence of false detection of returning PUs, i.e., we will erroneously assume that a PU has returned, when in fact the PU's channel is free. A simple way to characterize the occurrence of false alarms for already transmitting SUs is to use the average number of false alarms per a time unit, similar to the rate parameter of a Poisson process. We call this parameter the false alarm rate parameter λ_{FAR} [10, 11]. It is to be mentioned that in multi-channel systems with handoff capability (as studied here), an SU moving from its current operating channel (for example, due to false detection of a returning PU) will attempt to locate another free channel to continue its ongoing data transmission.

To protect reappearing PUs, SUs perform spectrum sensing on a continuous basis along with data transmission. Figure 1 presents the concept of simultaneous

*Correspondence: isam@ee.oulu.fi
[1] Department of Communications Engineering (DCE), University of Oulu, Oulu 90014, Finland
Full list of author information is available at the end of the article

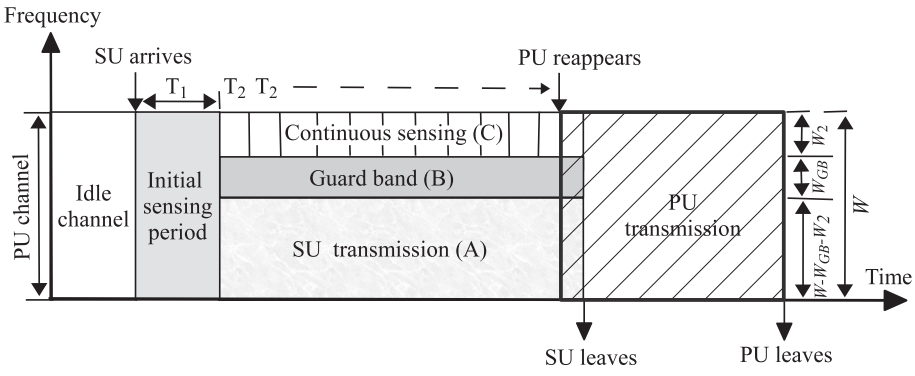

Fig. 1 Continuous sensing and data transmission

spectrum sensing and data transmission. When a new SU arrives at a channel for the first time, it senses the whole PU channel with a bandwidth W for T_1 seconds. After discovering that the channel is free, the SU starts data transmission over a bandwidth of $W - W_{GB} - W_2$. While the SU is transmitting data over the lower part of the PU channel, it continuously monitors the PU channel using the upper part with bandwidth W_2 to detect the presence of a returning PU. A guard band (GB) subchannel is used to prevent the leakage from SU's self-interference signal. The SU makes sensing decision every T_2 seconds. As a PU reappears (if correctly detected by the SU), the SU ceases its data transmission and leaves the channel.

Spectrum sensing errors impose several challenges into the design of CRNs and specially in models that employ simultaneous spectrum sensing and data transmissions. For example, the frequent occurrence of false alarm events is highly undesirable since it makes it challenging for SUs to fully utilize the spectrum opportunities and severely degrades their quality of service (QoS). The results reported in [12] have revealed the importance of investigating the effect of unnecessary spectrum handoff due to false alarms during spectrum sensing. Motivated by these issues, we develop a comprehensive CTMC analytical framework which models all related sensing factors that have not been fully accounted for in previous works. Our model can incorporate the effect of FAR as well as handling of the effect of the residual self-interference that is left over after SIC process. To our knowledge, the effect of the FAR on the operation of CRNs has not been investigated in the literature. The contribution of this paper can be summarized as follows:

- It motivates and develops a CTMC-based analytical framework that precisely evaluates the performance of CRNs. Unlike existing approaches, the proposed model thoroughly investigates the effect of FARs on the performance of CRNs. The model also takes into consideration the SUs residual self-interference as well as interference tolerance among PUs and SUs.
- It models the occurrence of FAR events as a Poisson process with parameter λ_{FAR} with a theoretical justification based on a shrinking Bernoulli process [13].
- It proposes a new performance evaluation measure, the SU self-termination probability. The proposed metric can precisely measure the percentage of SU calls that are terminated because of the FAR occurrence. The new metric also allows for measuring the SUs' ability of utilizing spectrum opportunities.
- Extensive simulations to validate the theoretical results.

We believe that the work presented in this paper contributes towards a better understanding and provides a new insight into the operation of CRNs and can be used to develop more accurate and realistic CRNs performance analysis models. The rest of the paper is organized as follows. Section 2 presents the related work. The system model is presented in Section 3. Section 4 contains a description of the continuous spectrum sensing and data transmission. Section 5 presents the CTMC-based analytical framework. In Section 6, we discuss performance evaluation metrics for the CRN. Section 7 summarizes results and provides comparison of simulation and theoretical results. Finally, Section 8 provides the conclusions and remarks on future work.

2 Related work

In recent years, several studies has been proposed to detect returning PUs in CRNs. In [14], the authors investigate the issues of how to maximize the overall discovery of opportunities in the licensed channels and how to minimize the delay in locating an idle channel in order to minimize interference on returning PUs. Similarly, the authors of [15] presented a dynamic spectrum access mechanism in a network where SUs do not have perfect knowledge of PUs' communication behavior. The interference issue has also been studied. However, this study only considered perfect spectrum sensing and a network with only

one PU. In [16], the authors consider a preemptive priority approach for the channel access where SUs must vacate their channels whenever the corresponding PUs appear. The work presented in [17] formulates a joint spectrum sensing and access problem as an evolutionary game by considering the mutual influence between spectrum sensing and access. Although the interference problem has been addressed in these works, the problem of the FAR has not been investigated.

In [18], continuous time Markovian process (CTMP) is used to model PU traffic in opportunistic spectrum access (OSA) systems. However, for analyzing SU's behavior, discrete time queuing was used. In contrary to our work, the underlying assumption made therein is that sensing and data transmission cannot be carried out simultaneously and therefore the SU has to periodically suspend its data transmission in order to perform spectrum sensing. The problems with this technique are the overheads associated with the scheduling and synchronization of the suspension periods among SUs as well as the frequent interruption in the SU's data transmission. Additionally, the SU can only detect a reappearing PU during the suspension period, even if the PU reappeared before the suspension period. This work also differs from our study because it only supports CRNs with one channel and the assumption that the spectrum sensing is perfect.

Simultaneous spectrum sensing and data transmission approach have been studied in [19–22]. The issue of self-interference due to transmitting and receiving in the same band has been studied in [23, 24]. In spite of considering the problem of unnecessary false alarms, the authors of [12, 25] did not investigate their effect on performance metrics such as blocking and termination probabilities. Furthermore, the authors of [26] analyzed different types of unreliable sensing for both incoming and ongoing SUs and their impact on the performance of CRNs without addressing the FAR.

Most of the existing CTMC models [27–29] do not cover all the aspects of the spectrum sensing and CRN operation and some important factors were not fully addressed. In our previous work [30], we analyzed the performance of CRNs using a CTMC framework that supports multi-channel, spectrum handoff, full-state dependent transition rates, and the ability to handle spectrum sensing errors. In this paper, we extend the analysis in [30] to capture the effect of the FAR and to handle the residual self-interference within the SU transceivers.

3 System model

We consider a CRN with N number of channels in which SUs are allowed to opportunistically utilize licensed spectrum bands with the constraint that the QoS of PUs remains at an acceptable level. There are two approaches for enabling PUs and SUs to coexist and share radio resources in CRNs: spectrum sharing (SS) and opportunistic spectrum access (OSA) [31]. In the SS model, SUs are allowed to transmit simultaneously with PUs on the same band. On the other hand, the OSA approach, which is more suitable for the model presented in this paper, allows SUs to access the licensed channels opportunistically when PUs are not present.

3.1 Primary user model

We assume that the primary channel occupancies are time varying alternating between idle and busy periods, and thus SUs must perform spectrum sensing continuously to detect the presence of returning PUs. PU connections arrive at the network according to a Poisson process at a rate of λ_1. The PU service rate which is assumed to be exponentially distributed is μ_1. We also assume that PUs can obtain primary channel occupancy information, for example, by accessing a core network that makes signaling or querying of the PUs' base station [32], and thus it is further assumed that PUs do not collide with each other [28].

We assume that both PUs and SUs have some interference tolerance T_{TOL} of how many seconds of interference they will tolerate before withdrawing from the system. If the PU interference tolerance time T_{TOL} is 0, no SU transmission is allowed [33]. We assume equal interference tolerance for both systems leading to both colliding users withdrawing from the system simultaneously. A similar assumption has been considered previously in [28].

3.2 Secondary user model

We assume that SU connections arrive at the network according to a Poisson process with λ_2. The SU service rate is assumed to be exponentially distributed with μ_2. During the absence of PUs, SUs can opportunistically access the free channels if they are not occupied by other SUs. We also assume that SUs are capable of broadcasting control messages on a common control channel (CCC) [34] to show their existence to neighboring SUs in the proximity. Therefore, SUs do not attempt accessing channels occupied by other SUs. Upon detection of the presence of a returning PU, a SU leaves its current channel and starts the spectrum handover process in order to find a new free channel. If the channel search process ends without finding a free channel, the SU terminates its call and leaves the network.

As illustrated in Fig. 1 and similar to the distributed (coordination function) interframe space (DIFS) operation in IEEE 802.11, the SU has to keep sensing the PU channel from the beginning of its transmission, since the PU can arrive at any time instant of a slot. This process forms a continuous sequence of sensing slots with length equals T_2. For example, if the PU appears in the middle of a time slot, then the first slot will not get full PU

energy, leading to a smaller detection probability than the later full slots. Since the first T_2 may be wasted, we assume that the first partial slot sensing never leads to detection, i.e., the detection probability is close to zero. Hence, we should detect the PU arrival during $T_{\mathrm{TOL}} - T_2$ seconds which corresponds to $\widehat{T_{\mathrm{TOL}}} = \left\lfloor \frac{T_{\mathrm{TOL}}-T_2}{T_2} \right\rfloor$ slots. Although partial slot sensing can enable the SU to perform sensing immediately after the arrival of the PU and hence have a prompt reaction to protect PUs, for the sake of simplifying the analysis, we consider only the full slot sensing by assuming that the detection process will begin from the first full time slot following the SU arrival.

4 Continuous spectrum sensing model

One possibility for implementing continuous sensing is to leave the upper part of the PU channel empty (i.e., free from SU transmissions) [35]. As shown in Fig. 1, we split the PU channel into three subchannels: (A) SU communication channel, (B) a sufficient vacant guard band to reduce the effect of SU's self-interference, and (C) SU sensing channel. When the PU is active, it uses the whole bandwidth (A+B+C) for its communication. The secondary user uses subchannel (A) for its communication. A reappearing PU can be detected by sensing, during ongoing SU transmission from the subchannel (C). It is obvious that a problem here is the self-interference due to the leakage of the SU's transmitted signal back to its sensing device. However, the emergence of a large variety of self-interference cancellation techniques [36–38] in the literature enabled efficient reduction in self-interference and therefore allowing radios to operate in full-duplex mode. For example, the authors of [39] present a method for canceling a passband self-interference signal using adaptive filtering in the digital domain. Therefore, in addition to the vacant guard band and bandpass filtering, self-interference cancellation has also been assumed to remove most of the residual self-interference. In this model, $q \in \{1, 2\}$ denotes an index with the interpretation that $q = 1$ if the spectrum sensing is carried out by incoming SUs and $q = 2$ if the spectrum sensing is performed by ongoing SUs.

4.1 Energy detector-based spectrum sensing

Without loss of generality, we consider that initial and ongoing spectrum sensing are done using an energy detector [9] with an integrate and dump operation mode as described in [10, 11]. The analysis techniques presented in this paper are generic and not limited to any particular detector, provided that the used detector can be mapped to false alarm probabilities, probability of detections, and false alarm rates. Let $y_q(t)$ denote the SU received signal process. We express the incoming SU received signal process in the form

$$y_1(t) = \begin{cases} n(t) & : H_0 \\ h_{\mathrm{PU}} s_{\mathrm{PU}}(t) + n(t) & : H_1, \end{cases} \tag{1}$$

and the ongoing SU received signal process can be formulated as

$$y_2(t) = \begin{cases} h_{\mathrm{SU}} s_{\mathrm{SU}}(t) + n(t) & : H_0 \\ h_{\mathrm{PU}} s_{\mathrm{PU}}(t) + h_{\mathrm{SU}} s_{\mathrm{SU}}(t) + n(t) & : H_1, \end{cases} \tag{2}$$

In Eqs. (1) and (2), $s_{\mathrm{PU}}(t)$ is the PU transmitted signal, $s_{\mathrm{SU}}(t)$ represents the leakage from the SU transmitted signal, $n(t)$ is the additive white Gaussian noise (AWGN), h_{PU} is the PU channel gain while h_{SU} represents the SU leakage signal gain, and t is the time. In the above equations, H_0 is the null hypothesis meaning that PU is not present in the sensed band, and H_1 represents the alternative hypothesis referring to the presence of the PU signal.

The received signal is filtered by a bandpass filter to remove the out-of-band and self-interference noise. The filtered signal is then squared by the squaring device and applied to the integrator. The integrator output Y_q (also denotes the decision variable of the energy detector) is sampled every T_q seconds. Then, the integrator is reset before integrating the next sample over the next T_q seconds. Finally, Y_q is compared with the decision threshold to decide about the presence of the PU. Let W_q denote the sensed bandwidth. Let γ_q denote the signal to noise ratio SNR and η_q denote the energy detection threshold. According to [9]

$$Y_q \sim \begin{cases} \chi^2_{2u_q} & \text{under } H_0 \\ \chi^2_{2u_q}(2\gamma_q), & \text{under } H_1, \end{cases}$$

where $\chi^2_{2u_q}$ is a chi-square distribution with $2u_q$ degrees of freedom (i.e., the time-bandwidth product $u_q = W_q T_q$) and $\chi^2_{2u_q}(2\gamma_q)$ is a non-central chi-square distribution with $2u_q$ degrees of freedom and a non-centrality parameter $(2\gamma_q)$. It has been shown in [40] that the probability of detection P_{Dq} and the false alarm probability $P_{\mathrm{FA}q}$ can be given as follows:

$$P_{Dq} = Q_{u_q}\left(\sqrt{2\gamma_q}, \sqrt{\eta}_q\right), \tag{3}$$

$$P_{\mathrm{FA}q} = \frac{\Gamma\left(u_q, \frac{\eta_q}{2}\right)}{\Gamma(u_q)}, \tag{4}$$

where $Q_{m(.,.)}$ is the generalized mth Marcum Q-function [41].

Referring to Fig. 1, where W represents the PU channel bandwidth. To obtain the received signal energy, let P_{PU} denote the PU transmitted signal power. Let also N_0 denote the one-sided power spectrum density (PSD). Let T_1 denote the incoming SU initial sensing time. Assuming

that the PU signal power is uniformly distributed over the PU channel, then the incoming SU signal energy within the initial sensed area can be obtained as

$$E_{S1} = P_{\mathrm{PU}} T_1 \tag{5}$$

and the initial sensing SNR is then obtained with

$$\gamma_1 = \frac{E_{S1}}{N_0} \tag{6}$$

Similarly, we can obtain the signal energy within the ongoing SU sensed area with a sensing time duration T_2 as

$$E_{S2} = P_{\mathrm{PU}} T_2 \frac{W_2}{W} \tag{7}$$

Although we use guard band, bandpass filtering, and self-interference cancellation to eliminate the effect of SU leakage signal, we assume that the SU self-interference has not been fully removed. To handle the effect of any remaining self-interference, we follow the results presented in [42] to model the residual interference. Let assume that the SU operate with a single-antenna full-duplex transceiver. Let α_{SU} denote the SU's residual interference distortion factor. By using Eq. (2), the effective ongoing sensing SNR can be expressed as [42]

$$\gamma_2 = \frac{E_{S2}}{N_0(1+\alpha_{\mathrm{SU}})} \tag{8}$$

In continuous spectrum sensing with full-duplex communication, the consideration of self-interference is particulary important since the self-interference can affect the sensing outcome and degrade SUs performance. Although the SU self-interference signal can have nonzero mean, it has been been assumed in the majority of related works to have a zero mean. For instance in [43], the authors mentioned that in practical full-duplex systems, the self-interference cannot be completely canceled, such that the signals received at each node is a combination of the signal transmitted by the other source, the residual self-interference (RSI), and the noise. They also assume that the RSI can be typically modeled as zero-mean additive white Gaussian noise (AWGN). The work reported in [42] assumed that the Gaussian distortion and noise follows central chi-square distribution in the absence of PU signals but potentially including RSI and noncentral chi-square distribution when PU signal is present.

Self-interference mitigation in full-duplex MIMO relays has been investigated in [23] where the authors focused on minimizing the residual loop interference so that it can be regarded as additional relay input noise. They assumed that all signal from the relay output to the relay input (including loop interference (LI) signal) and noise vectors have zero mean. Furthermore, the authors of [44–46] assumed that the SU self-interfering signal before carrying out self-interference suppression (SIS) to be a zero-mean random signal with self-interference channel coefficient equal one. In [47], the residual self-transmitted signal is modelled with circular symmetric complex Gaussian variables. Following the common practice in existing models, the use of the assumption that SU's leakage signal can be zero mean and follows central chi-square distributions is justified and can be hold in order to take into account the RSI signal and perform the analysis.

It should be noted that when we use a dedicated part of the bandwidth (subchannel C) for continuous sensing, the effect of the residual interference becomes much lower than when we use the full bandwidth for simultaneous sensing and transmission. Each incoming SU correctly detects channel occupancy with probability P_{D1}, and falsely classifies a free channel as occupied with P_{FA1}. Similarly, each SU with ongoing calls detects the arrival of a PU with probability P_{D2} and falsely classifies a free channel as occupied with P_{FA2}. The corresponding misdetection probabilities for incoming and outgoing SUs are $P_{M1} = 1 - P_{D1}$ and $P_{M2} = 1 - P_{D2}$, respectively. The detection probability P_{D2} refers to the probability of detecting incoming PU during the first $\widehat{T_{\mathrm{TOL}}}$ full slots of its arrival, instead of the per-slot detection probability. If the per-slot detection probability is denoted as z then $P_{D2} = 1 - (1-z)^{\widehat{T_{\mathrm{TOL}}}}$. This does not affect the FAR process since one per-slot false alarm event is enough to initiate the spectrum handoff and channel searching process. Modeling of partial slot sensing is left for future work.

4.2 Poisson process approximation

We model the occurrence of the false alarm at each sensing decision with the Bernoulli process. The energy detector makes only one sensing decision in each slot which results into a binary variable (0 or 1). Since the sensing decisions with only white Gaussian noise present are independent, the resulting binary output of the sensing clearly follows the Bernoulli process (i.e., independent and identically distributed process generating 1 and 0 s), and the Bernoulli parameter corresponds to the probability of FAR occurrence (binary output 1) in each spectrum sensing decision.

At each spectrum sensing decision epoch T_2, a false alarm occurs with probability P_{FA2} and does not occur with probability $1 - P_{\mathrm{FA2}}$, independently of the decision outcome of the last sensing period. The λ_{FAR} parameter is the product of the decision rate and the false alarm probability [10, 11, 48]. Therefore, λ_{FAR} is given by P_{FA2}/T_2. Let us assume that the sensing interval T_2 is short and therefore we assume that the decision rate given by $1/T_2$ is large, and that the false alarm P_{FA2} is small as otherwise there would be too many false alarms for successful SU operation. Then, the arrival process of false alarms can be

approximated by a Poisson process as a limit of a shrinking Bernoulli process [13] with parameter λ_{FAR}.

5 Continuous time Markov chain model (CTMC)

We consider a two-dimensional continuous time Markov chain (CTMC) to describe the CRN system. At any time, the system state is determined by (i,j) where i represents the number of channels occupied by PUs and j represents the number channels occupied by SUs with restriction that $0 \leq i \leq N$, $0 \leq j \leq N$, $0 \leq i+j \leq N$. Let $i\mu_1$ and $j\mu_2$ denote the the service completion time for PUs and SUs, respectively. The transition rate from state (i,j) to state (h,l) is given by $T^{(i,j)}_{(h,l)}$. Note that the parameter λ_{FAR} affects all state transitions from states with the number of SUs $j > 0$. As the number of channels increases, the number of states of the CTMC grows exponentially. Since the transition rates depend on the system states, the large number of states combined with the channel searching process under imperfect sensing conditions would make it not trivial to compute the state transition rates. Because it is impractical to present a state transition diagram for a CRN with an arbitrary number of channels, we present an illustrative example in Fig. 2 which shows the allowable state transitions from and to state (1,1) in a Markov chain with three channels.

As an example, consider a CRN with three channels denoted by $C1$, $C2$, and $C3$. Let us assume that channel $C1$ is occupied by an PU, channel $C2$ is occupied by a SU, and the last channel $C3$ is free. The Markov chain is in state (1,1). We now explain a series of events that trigger the system to move from state (1,1) to state (0,0). State (0,0) indicates that all channels are free. On the occurrence of λ_{FAR}, the SU leaves $C2$ and starts the channel searching process. There are two channel selection possibilities for the SU for continuing its data transmission. The SU can first select $C1$ with probability 1/2 and then misdetect the presence of the PU on $C1$ with probability P_{M1}. The second possibility is to select $C3$ with probability 1/2, then falsely classify the free channel as occupied by the PU with a false alarm probability P_{FA1}, and finally misdetect the presence of the PU on $C1$ with probability P_{M1}. Both selections lead the SU to collide with the PU, and eventually both of them leave the network. Combining all these events, the transition rate from state (1,1) to state (0,0) can be obtained by $\frac{\lambda_{\mathrm{FAR}} P_{M1}}{2}(1+P_{\mathrm{FA1}})$.

Another example is the transition from state (1,1) to state (2,0). This happens with the arrival of a PU with rate λ_1 and with probability 1/2 to channel $C2$ which is occupied by the SU. The SU correctly detects the presence of the PU with detection probability P_{D2} and vacates the channel. After leaving the channel, the SU has two possibilities with probability 1/2 for each. The SU first falsely classifies the free channel $C3$ as being occupied by a PU with false alarm probability P_{FA1} and then detects the presence of the PU in channel $C1$ with probability P_{D1}, ending up leaving the network. The other possibility is that the SU correctly detects the existence of the PU in channel $C1$ with probability P_{D1} and then erroneously classifies the free channel $C3$ as occupied by a PU with false alarm probability P_{FA1}. The resulting transition rate is $\frac{\lambda_1 P_{D2} P_{D1} P_{FA1}}{2}$. Proceeding in a similar manner, the transition rates to and from the remaining states can be obtained.

5.1 Generalization of the CTMC

The goal of this section is to extend the results presented previously to describe a CRN with an arbitrary number of channels N. When N is large, constructing a state transition diagram and finding a solution to the corresponding balance equations is complicated and time consuming. Similar to [30], we use a recursive method to calculate the state transition rates to and from all different states of the CTMC representing the CRN network. The state transition rates are used to get all the possible balance equations. Recalling that the number of PUs is denoted by i and the number of SUs is denoted by j. Let us also assume that the number of free channels is denoted by k which is given by $k = N - i - j$.

It is important to notice that the state transition rates presented in this paper are different from those defined in [30] for several reasons: (1) the inclusion of the effect of the FAR in the CTMC. (2) In our previous work [30] we assumed that ongoing SUs perfectly detect the arrival of PUs and that there are no false alarms during ongoing data transmission. However, in this paper, we assume that SUs with ongoing connections do not perfectly detect the arrival of PUs and also that the false alarm probability during ongoing calls is not negligible. With this assumption, ongoing SUs detect PU arrivals with P_{D2} where P_{D2} is an arbitrary value between 0 and 1 and that the false alarm probability during ongoing calls equal P_{FA2} which is also an arbitrary value. Note that this is a more realistic assumption for practical CRNs and represents a significant improvement over our previous work [30] that leads to obtaining accurate state transition rates and state probabilities. (3) Because of the false alarms during ongoing sensing, we require a new state transition that defines the transition from state (i,j) to state $(i-1,j-1)$, with $i > 0$ and $j > 0$. In addition to state transitions because of the FAR events, we refer the reader to [30] for details concerning the other different events that trigger state transitions. All possible state transition types are described as follows:

- Transition type 1: $(i,j) \rightarrow (i,j+1)$. This transition defines the increase in the number of SU by one and can be obtained by

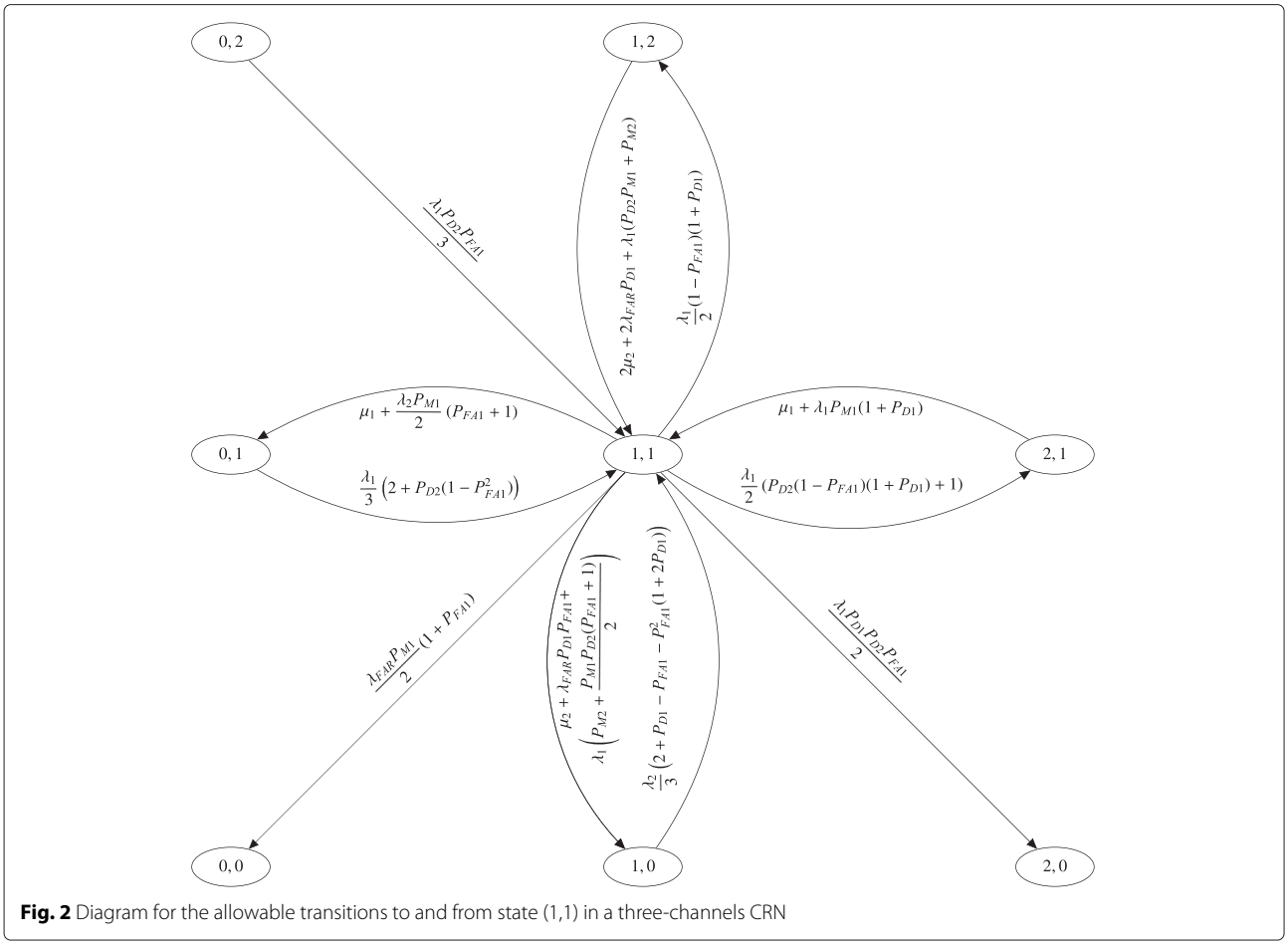

Fig. 2 Diagram for the allowable transitions to and from state (1,1) in a three-channels CRN

$$f(i,k) = \frac{k}{i+k}(1 - P_{\mathrm{FA1}}) + \frac{k}{i+k} P_{\mathrm{FA1}} f(i,k-1) + \frac{i}{i+k} P_{D1} f(i-1,k) \tag{9}$$

where function $f(.)$ is used to define the increase in the number of SUs by 1 [30]. P_{D1} and P_{FA1} have been defined earlier to denote the initial sensing's detection and false alarm probabilities. They have been used to obtain more accurate state transition rates and state probabilities in comparison to results obtained in [30]. The overall state transition rate for this case is given by $\lambda_2 f(i,k)$

- Transition type 2: $(i,j) \rightarrow (i-1,j)$. This transition defines the decrease in the number of PUs by one. We use the recursive function $g(.)$ [30] to define this transition

$$g(i,k) = \frac{i}{i+k} P_{M1} + \frac{i}{i+k} P_{D1} g(i-1,k) + \frac{k}{i+k} P_{\mathrm{FA1}} g(i,k-1), \tag{10}$$

where P_{M1}, P_{D1}, and P_{FA1} denote the initial sensing's misdetection, detection, and false alarm probabilities, respectively. The overall state transition rate for this case can be obtained by $i\mu_1 + \lambda_2 g(i,k)$ [30].

- Transition type 3: $(i,j) \rightarrow (i+1,j)$. This transition is given by

$$T_{(i+1,j)}^{(i,j)} = \lambda_1 \left(\frac{N-i-j}{N-i}\right) + \frac{j\lambda_1 P_{D2}}{N-i} f(i, N-i-j) \tag{11}$$

to reflect the increase in the number of PUs by one.

- Transition type 4: $(i,j) \rightarrow (i,j-1)$. The state transition rate for decreasing the number of SUs by one is given by

$$T^{(i,j)}_{(i,j-1)} = j\mu_2 + \lambda_1 P_{M2}\frac{j}{N-i} + j\lambda_{\mathrm{FAR}}\left(1 - f(i,N-i-j) - g(i,N-i-j)\right) + \lambda_1 P_{D2}\frac{j}{N-i}g(i,N-i-j) \tag{12}$$

- Transition type 5: $(i,j) \rightarrow (i+1,j-1)$. The state transition rate for this case is given by

$$T^{(i,j)}_{(i+1,j-1)} = \left(\lambda_1 P_{D2}\frac{j}{N-i}\right) \times \left(1 - f(i,N-i-j) - g(i,N-i-j)\right) \tag{13}$$

- Transition type 6: $(i,j) \rightarrow (i-1,j-1)$. The number of PUs is decreased by one and the number of SUs is decreased by one. This transition occurs if after the occurrence FAR, the SU ends up colliding with a PU. We get the transition rate as

$$T^{(i,j)}_{(i-1,j-1)} = j\lambda_{FAR}\left[g(i,N-i-j)\right] \tag{14}$$

$$\mathrm{SU_{FTP}} = \frac{\left[\sum_{i=0}^{N-1}\sum_{j=1}^{N-i}\boldsymbol{\pi}_{(i,j)}\left(T^{(i,j)}_{(i+1,j-1)}\right) + \sum_{i=0}^{N-1}\sum_{j=1}^{N-i}\boldsymbol{\pi}_{(i,j)}\left(T^{(i,j)}_{(i,j-1)} - j\mu_2\right) + \sum_{i=1}^{N-1}\sum_{j=1}^{N-i}\boldsymbol{\pi}_{(i,j)}\left(T^{(i,j)}_{(i-1,j-1)}\right)\right]}{\lambda_2} \tag{15}$$

$$\mathrm{PU_{FTP}} = \frac{\left[\sum_{i=1}^{N}\sum_{j=0}^{N-i}\boldsymbol{\pi}_{(i,j)}\left(T^{(i,j)}_{(i-1,j)} - i\mu_1\right) + \sum_{i=0}^{N-1}\sum_{j=1}^{N-i}\boldsymbol{\pi}_{(i,j)}\left(T^{(i,j)}_{(i,j-1)} - j\mu_2\right) + \sum_{i=1}^{N-1}\sum_{j=1}^{N-i}\boldsymbol{\pi}_{(i,j)}\left(T^{(i,j)}_{(i-1,j-1)}\right)\right]}{\lambda_1\left(1 - \boldsymbol{\pi}_{(N,0)}\right)} \tag{16}$$

5.2 Construction of state transition rate matrix and computation of the steady state probability vector

Let $\mathbf{Q}$ denote the state transition rate matrix (also known as infinitesimal generator) of the CTMC. Let $\boldsymbol{\pi}$ denote the steady state probability vector with $\boldsymbol{\pi}_{(i,j)}$ denoting the probability that the system is in the steady state (i,j). When the system is in the steady or equilibrium state, the normalization condition is given by $\sum_{i=0}^{N}\sum_{j=0}^{N}\boldsymbol{\pi}_{(i,j)} = 1$ [49] with the condition that $0 \leq i \leq N$, $0 \leq j \leq N$, and $0 \leq i+j \leq N$. Let D equals the total number of states in CTMC. We map the elements of the steady state probability vector $\boldsymbol{\pi}_{(i,j)}$ from state to index by assigning a unique integer index to identify each state. Therefore, the steady state probability vector can be represented as $\boldsymbol{\pi} = (\pi_1, \pi_2, ..., \pi_D)$ and the normalization condition is given by $\sum_d \boldsymbol{\pi}_d = 1$. The steady state probabilities of the CTMC can be found by applying the following procedure:

- Step 1: Solve the recursive Eqs. (10–15) to obtain the state transition rates.
- Step 2: Drive the balance equations using the rule that incoming transition rates to each state must equal outgoing transition rates from that state [50].
- Step 3: Use the balance equations to build the infinitesimal generator matrix $\mathbf{Q}$. All elements not on the main diagonal of $\mathbf{Q}$ represents state transition from one state to another. The elements on the main diagonal of $\mathbf{Q}$ make the sum of the elements in the respective row equal zero [51].
- Step 4: Apply the normalization condition $\sum_d \boldsymbol{\pi}_d = 1$
- Step 5: Solve the system of linear equations $\boldsymbol{\pi}\mathbf{Q} = 0$ to obtain the CTMC's steady state probabilities.

Each element in the steady state probability vector $\boldsymbol{\pi}$ represents the percentage of time that the system spends in that state.

Since the number of states of the CTMC grows exponentially with the number of the channels in the network, it would be impossible to derive the CTMC transition rates by hand for large number of states. In this sense, the utilized recursive approach solves one part of this problem. However, the number of states is still exponential, which lead to higher memory and processing time requirements when the number of channels increases since the full-state transition matrix is used to obtain exact results. With very large number of channels, approximation solutions with reduced number of channel states would be beneficial. In the literature, some approximation methods have been presented for CTMCs with a large number of states [51, 52]. The results presented in this paper have been obtained using the exact full CTMC. However, when the number of channels is very large which brings some inefficiency, we can apply approximate solutions of large CTMCs to overcome this problem [51, 52].

6 Performance evaluation measures

In order to measure the performance of the CRN, we define several performance evaluation measures: secondary forced termination probability (SU_{FTP}), primary forced termination probability (PU_{FTP}), and secondary self termination probability (SU_{STP}). Those performance metrics are calculated by using the state transition rates and the steady state probabilities $\boldsymbol{\pi}_{(i,j)}$ and state

transition rates derived in the previous section. The reader is referred to [30] for more details on the definition and derivation of other performance metrics such as secondary successful probability (SU_{SP}), primary blocking probability (PU_{BP}), secondary blocking probability (SU_{BP}), as well as system resource utilization.

6.1 Secondary forced termination probability (SU_{FTP})

The secondary forced termination probability, denoted by SU_{FTP}, is the probability of terminating SU calls because of SU's failure to find a new free channel after moving from its current channel. The SU_{FTP} is calculated and defined by Eq. (15). It reflects the ratio of terminated SUs' call to total SU call arrivals λ_2.

6.2 Primary forced termination probability (PU_{FTP})

The primary forced termination probability, denoted by PU_{FTP} and given by Eq. (16), is calculated as the ratio of terminated PU calls because of collisions with SUs to the total primary call arrivals λ_1.

6.3 Secondary self termination probability (SU_{STP})

Here, we introduce a new performance metric that measures the secondary self-termination probability. The motivation of proposing this new metric starts with the fact that in CRNs, the occurrence of false alarms is of critical importance since significant amount of SUs' calls could be terminated because of FARs. The new metric helps in accurately determining the percentage of SUs' connection terminated due to SUs' own errors. By identifying this metric, it allows for measuring the SUs' ability of utilizing spectrum opportunities and helps in designing CRNs by setting correct spectrum sensing parameters. The metric determines the ratio of terminated SU calls because of FAR occurrence to the total secondary call arrivals λ_2. As mentioned earlier, upon λ_{FAR} arrival, an SU has to terminate its own active call if it finishes the channel searching process without finding a new idle channel. The SU_{STP} can be calculated as:

$$\mathrm{SU_{STP}} = \frac{\sum_{i=0}^{N-1}\sum_{j=1}^{N-i} \boldsymbol{\pi}_{(i,j)} \left(\overline{T}^{(i,j)}_{(i,j-1)}\right)}{\lambda_2} \tag{17}$$

where $\overline{T}^{(i,j)}_{(i,j-1)}$ represents the portion of the transition rate from state (i,j) to state $(i,j-1)$ that occur because of the λ_{FAR}.

7 Simulation and numerical results

In this section, we report results obtained both through theoretical analysis and simulations. We conduct simulations with MATLAB using an event-based approach and Poisson arrival processes. The parameters in simulations and theory are chosen as follows: We set the primary licensed bandwidth as 20 MHz, the initial sensing bandwidth is 20 MHz meaning that a SU carries out spectrum detection over the whole spectrum. However, the continuous sensing bandwidth is chosen to be 2 MHz. The initial sensing time = 20 μs. We set the primary and secondary service rates as $\mu_1 = \mu_2 = 4$. PU signal power is −91 dBm. The PU power has been set to a low level since SUs should be able to detect even weak PUs signals. The noise level is −160 dBm/Hz. To include the effect of the residual interference signal, we set the interference distortion factor to 0.1. We present plots for different performance metrics. It can be observed from all plots that the analytical results are in excellent agreement with the simulation results, which demonstrates the accuracy and validity of the CTMC analytical model.

7.1 ROC curves

The receiver operating characteristic (ROC) for both initial and continuous spectrum sensing is shown in Fig. 3. For continuous spectrum sensing, it can be clearly seen that better detection performance is achieved when large values of continuous sensing durations are used. However, for initial sensing, small initial sensing time T_1 is enough for good detection level. This improved initial detection performance can be attributed to the fact that incoming SUs perform spectrum sensing over the whole PU bandwidth and hence their time bandwidth product is improved.

The impact of the residual interference distortion factor α_{SU} on the detection and false alarm probabilities is demonstrated by the ROC curves shown in Fig. 3. The SNR value for the initial sensing is 19 dB. However, the SNR values for the continuous sensing vary depending on the spectrum sensing time duration T_2 that affects the time bandwidth product. We assume that the PU signal power is uniformly distributed over the PU channel. It can be seen that the residual interference affects the ROC curves, as the ROC performance drops significantly with increases in α_{SU} values. We can also see from the figure that the curve for the initial sensing with spectrum sensing time duration $T_1 = 10$ μs is identical with the curve for continuous sensing with spectrum sensing time duration $T_2 = 100$ μs and $\alpha_{\mathrm{SU}} = 0$. This is due to the fact that their time bandwidth products are the same and equal to 200. Figure 3 also shows the effect of the residual interference distortion factor α_{SU} on the false alarm and detection probabilities.

7.2 Effect of the interference tolerance $\widehat{T_{\mathrm{TOL}}}$

We start the analysis by investigating the impact of the PU interference tolerance on the performance of the CRN. We tested the cases of $\widehat{T_{\mathrm{TOL}}} = 0, 1, 2, 3, 4, 5$ slots. By recalling the fact that PU detection starts from the first full

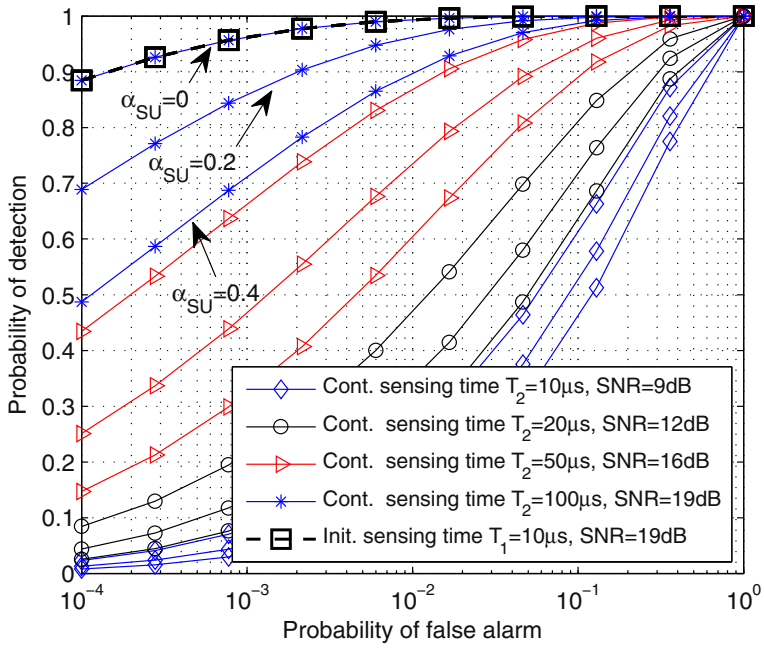

Fig. 3 ROC curve for initial and continuous spectrum sensing

$\widehat{T_{\mathrm{TOL}}}$ slots, if $\widehat{T_{\mathrm{TOL}}} = 0$, PUs tolerate only very little interference from an SU, and strict interference constraints should be satisfied. This means that the SU should leave the channel immediately upon the arrival of a PU. However, in practice, this is not possible since the SU user needs some sensing time to detect the presence of the PU. In Fig. 4, we compare the PU successful probability PU_{SP} for different values of T_{TOL} and against the PU arrival rate λ_1. We can observe from the figure the improvement in PU performance as we relax the interference constraint by increasing $\widehat{T_{\mathrm{TOL}}}$. We can also observe that the PU_{SP} drops significantly when $\widehat{T_{\mathrm{TOL}}} = 0$. However, when $\widehat{T_{\mathrm{TOL}}}$ is sufficiently large, PU performance starts to improve, indicating that SUs are getting enough sensing time to complete the process of detecting incoming PUs. This implies that the $\widehat{T_{TOL}}$ has to be chosen in a way that meets the PUs interference constraint, and at the same time also maximizes the CRN performance. Figure 4 also presents the impact of the primary arrival rate λ_1 on the CRN's performance in term of PU_{SP}. It can be easily seen that there are peak values in PU_{SP} curves. As λ_1 increases, the PU_{SP} improves. However, as λ_1 become large, most of the channels will be occupied by PUs, thus increasing the possibility of collisions with SUs who move away from their channels because of the λ_{FAR}.

Figure 5 confirms what we asserted above regarding the impact of $\widehat{T_{\mathrm{TOL}}}$ on the PU performance. While varying λ_1 from 1–10, the figure compares primary forced termination probability PU_{FTP} for each T_{TOL} value. It can be observed that PU_{FTP} monotonically decreases with increasing λ_1. It is also evident that the PU_{FTP} decreases with the increase of the $\widehat{T_{\mathrm{TOL}}}$. The reason behind this trend can be attributed to the fact that employing small $\widehat{T_{\mathrm{TOL}}}$ reduces the SUs capability of correctly detecting incoming PUs. In such a case, SUs collisions with incoming PUs increases forcing PUs to leave the network and hence increasing the PU_{FTP}.

In Fig. 6, we plot the secondary self termination probability SU_{STP} against λ_1 for different values of $\widehat{T_{TOL}}$. The figure shows that increasing $\widehat{T_{TOL}}$ can result in a significant SU performance degradation. For example, when $\widehat{T_{TOL}} = 0$, SUs collide with incoming PUs, making life easier for other secondary users since they could find free channels more easily. On the one hand, when λ_1 is small, PUs will have a smaller network resource share, leaving more opportunities for SUs. For example, SUs who leave their channels due to λ_{FAR} could find free channel and therefore reduce the SU_{STP}. On the other hand, when λ_1 is large, most of the channels will be occupied by PUs, leaving smaller network resources for SUs opportunistic access. In this case, the effect of SU_{STP} is more noticeable since with FAR occurrence (which trigger SUs to leave their channels), SUs either correctly detect the presence of PUs or collide with them. In both causes this leads to an increase in the SU_{STP}. Intuitively, PUs are better protected by employing large $\widehat{T_{\mathrm{TOL}}}$ as it provides SUs with enough sensing time to complete the detection process.

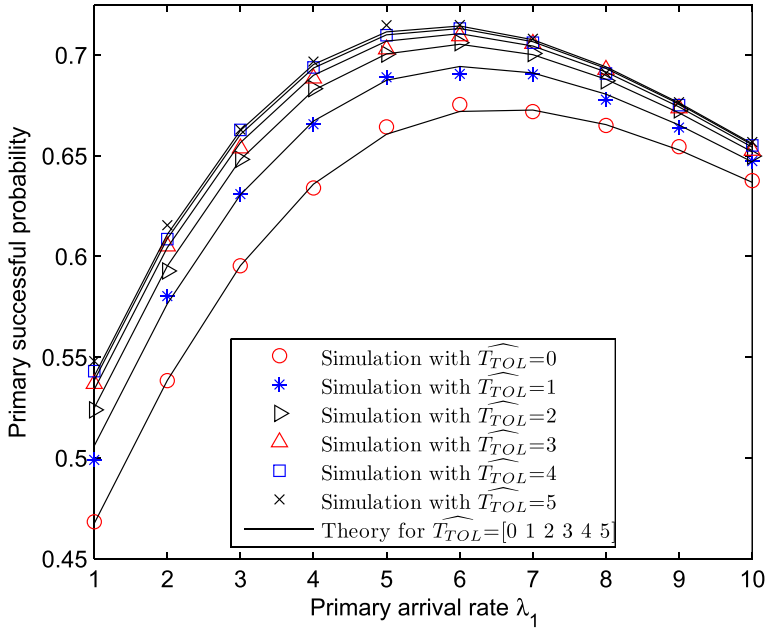

Fig. 4 Primary successful probability, $\lambda_2 = 3.5$, $\mu_1 = \mu_2 = 4$, $N = 3$

7.3 Effect of the false alarm rate

Figure 7 shows the effect of λ_{FAR} on the primary forced termination probability PU_{FTP} for different number of channels N. It can be seen from Fig. 7 that PU_{FTP} curves for different N have unique minimums at different λ_{FAR}s. The minimum points represent the optimum sensing parameters for SUs that would strongly protect PUs against forced connection termination. According to Fig. 7, the PU_{FTP} decreases with the increase in λ_{FAR} until it reaches the minimum point after which it starts to monotonically increase. On the one hand, too low λ_{FAR} reduces the PU's performance. The degradation in

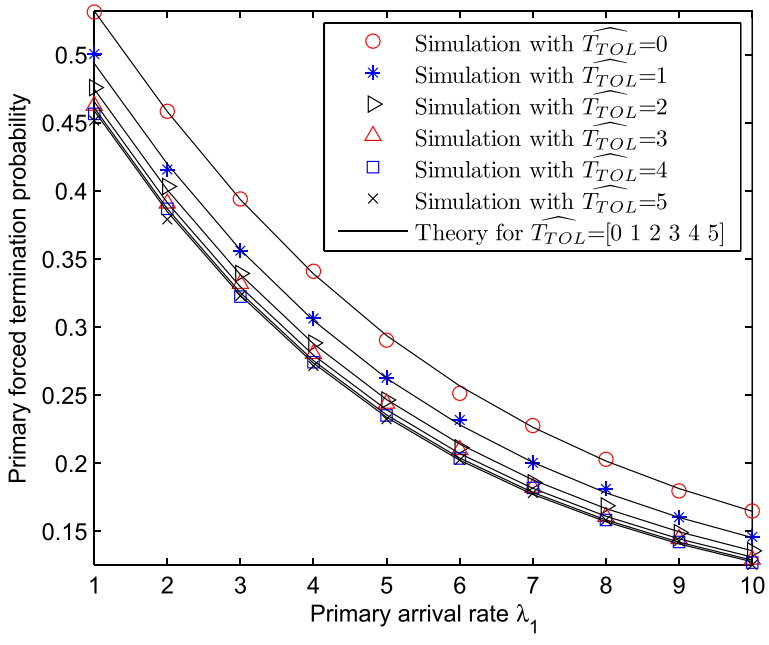

Fig. 5 Primary forced termination probability, $\lambda_2 = 3.5$, $\mu_1 = \mu_2 = 4$, $N = 3$

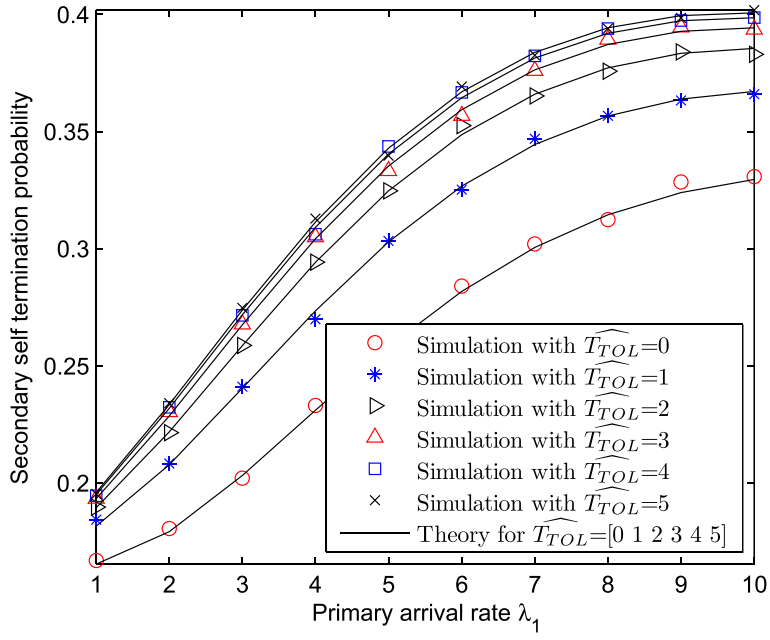

Fig. 6 Secondary self termination probability, $\lambda_2 = 3.5$, $\mu_1 = \mu_2 = 4$, $N = 3$

PUs performance is due to the fact that small values of λ_{FAR} leads to small P_{D2}, and therefore existing SUs frequently collide with incoming PUs and thereby increase PU_{FTP}. On the other hand, with high values of λ_{FAR} (and consequently high P_{D2}), it would be easy for SUs to detect incoming PUs and therefore they can avoid collision with them. However, too high λ_{FAR} is not good since SUs initiate unnecessary spectrum handoffs, leading to sharp increases in PU_{FTP}. As shown in the figure, the gap between PU_{FTP}'s curves shrinks as N increases. This

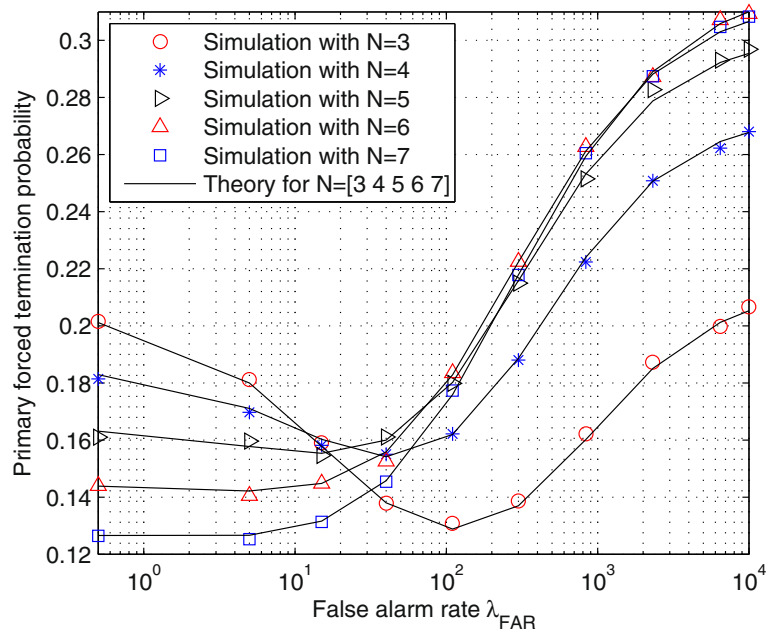

Fig. 7 Primary forced termination probability, $\lambda_1 = 7$, $\lambda_2 = 3.5$, $\mu_1 = \mu_2 = 4$, $\widehat{T_{\text{TOL}}} = 1$

reflects the fact that when N is sufficiently large, most of the channels are occupied by PUs because $\lambda_1 > \lambda_2$, and the combined effect of λ_{FAR}, P_{M2} and P_{M1} forces some PUs to terminate their calls. With further increases in N, the effect of λ_{FAR} on PU_{FTP} is flat, as there would be enough radio resources to meet SUs demands. After SUs avoid incoming PUs and initiate a handoff and channel switching process, SUs will most likely find new free channels and hence will not harm existing PUs as there are more channels to accommodate them.

Figure 8 presents the effect of λ_{FAR} on the secondary self termination probability SU_{STP} for different number of channels N. It can be seen that there are peak values in the SU_{STP} curves. The following explanation is related to this behavior: on the one hand, when λ_{FAR} is relatively low, SU_{STP} increases with the increase in λ_{FAR}, until it reaches the peak value and then starts to decline. The degradation in SU performance can be explained by the fact that as λ_{FAR} increases, a growing number of SUs leave their current channels. If they cannot find new free channels elsewhere they terminate their calls, and thereby increase the SU_{STP}. On the other hand, when λ_{FAR} is relatively large, the detection probability P_{D2} improves, which enables SUs to detect incoming PUs and move away from their channels. Hence, the proportion of SUs in the system is reduced, leading to a decrease in the SU_{STP}. It came as no surprise that increasing N greatly influences the SU_{STP}. When N is small, it would not be easier for SUs who initiate spectrum handoff to find new free channels to move to and the SUs have to leave the network. This results in a sharp increase in SU_{STP}.

In Fig. 9, for several values of N, we investigate the effect of λ_{FAR} on the primary successful probability PU_{SP}. The plot shows when λ_{FAR} is low; increasing λ_{FAR} slightly increases PU_{SP} until it reaches some (flat) peak points. The increase is a reflection of the improved detection P_{D2}. As can be observed from Fig. 10, increasing λ_{FAR} has an obvious negative impact on the secondary successful probability SU_{SP}. The reason for the reduction in SU_{SP} is that when λ_{FAR} is high, SUs increasingly initiate unnecessary spectrum handoff processes. SUs also initiate spectrum handoff processes if they detect the arrival of returning PUs. If SUs cannot find new channels, even though there are some free channel(s), they are forced to terminate their own connections and hence reducing SU_{SP}. The results shown in Fig. 10 indicate that SU optimal performance is when λ_{FAR} is close to zero. However, in practice, this value means SUs do not perform spectrum sensing and therefore cannot be used since too low λ_{FAR} leads to poor PU performance. Results shown in Fig. 7 confirm that low λ_{FARs} are not the best for PUs performance as they do not satisfy their QoS/interference constraint. Note that in order to improve network performance, there is a critical sensing tradeoff to be made. This result is a good motivation and illustrates the significance for optimizing detection parameters such that the effects of the λ_{FAR} can be kept within limits that would not harm PUs.

Figure 11 shows the influence of λ_{FAR} on the system resource utilization for different number of channels. When λ_{FAR} is small, SUs do not frequently initiate handoff processes and the effect of λ_{FAR} remains flat. However, as

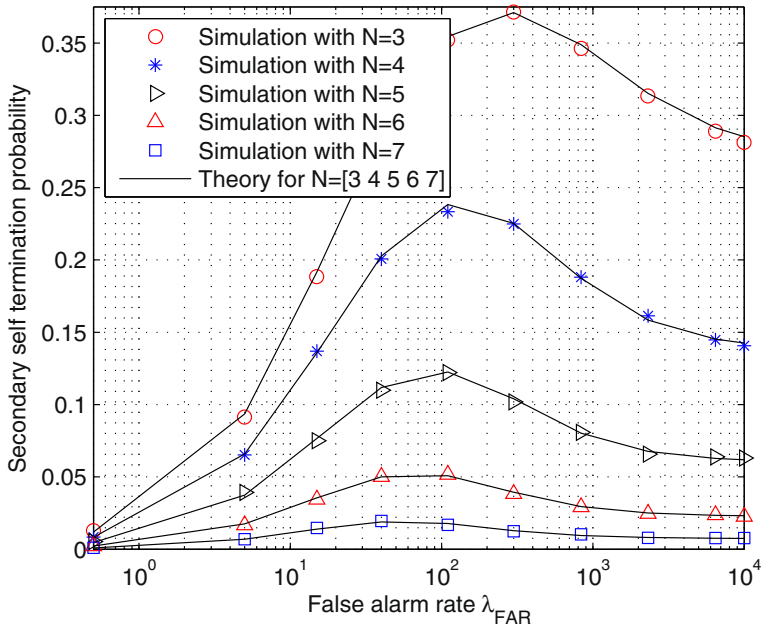

Fig. 8 Secondary self termination probability, $\lambda_1 = 7, \lambda_2 = 3.5, \mu_1 = \mu_2 = 4, \widehat{T_{\mathrm{TOL}}} = 1$

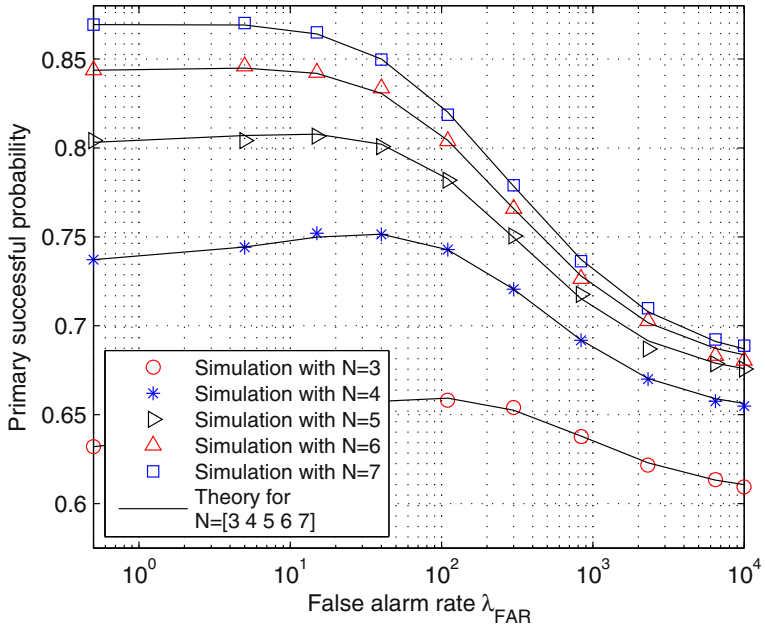

Fig. 9 Primary successful probability, $\lambda_1 = 7, \lambda_2 = 3.5, \mu_1 = \mu_2 = 4, \widehat{T_{\text{TOL}}} = 1$

λ_{FAR} increases, a growing number of SUs terminate their calls if they cannot find other free channels. This explains the reduction in the system resource utilization. As illustrated in Fig. 11, PUs' own resource utilization is lower than the overall system resource utilization. However, at high λ_{FAR}, PUs' and system resource utilization get closer. This indicates that SUs do not complete their service when λ_{FAR} is too high and the network resource is mainly utilized by PUs.

7.4 Performance under perfect spectrum sensing

The effect of perfect sensing on system resource utilization is shown in Fig. 12 where we plot a set of curves showing network resource utilization versus the secondary

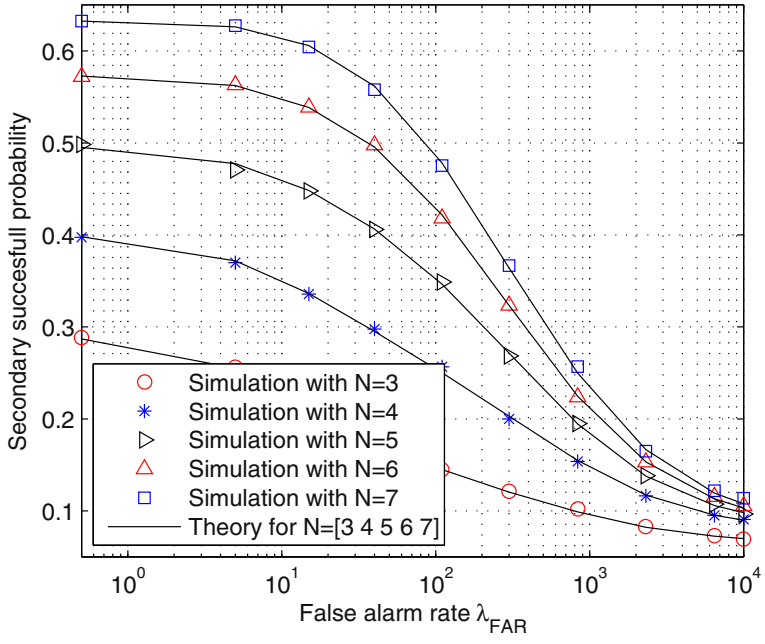

Fig. 10 Secondary successful probability, $\lambda_1 = 7, \lambda_2 = 3.5, \mu_1 = \mu_2 = 4, \widehat{T_{\text{TOL}}} = 1$

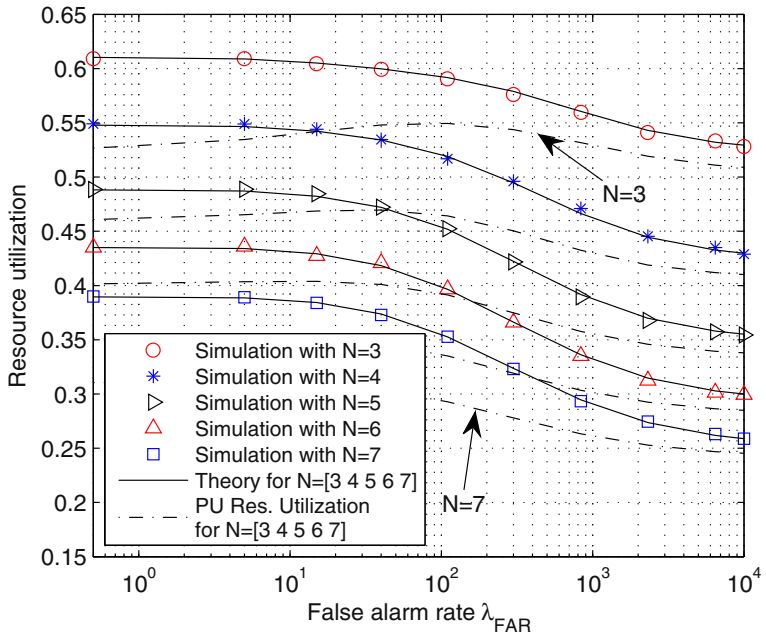

Fig. 11 System resource utilization, $\lambda_1 = 7, \lambda_2 = 3.5, \mu_1 = \mu_2 = 4, \widehat{T_{TOL}} = 1$

arrival rate λ_2 for different number of channels N. The dash-dotted curves depict the CRN performance when SUs operate without sensing errors. It can be observed that, due to the absence of false alarms, network resources are better utilized. In this case, all unoccupied PUs' channels can be opportunistically utilized by SUs. This effect is more noticeable when λ_2 is high. On the other hand, sensing errors can severely reduce the network resource utilization. The impact of the resource underutilization can be reflected in the huge gap between the resource utilization curves. As λ_2 increases, a growing number of SUs gain network access. However, λ_{FAR} prevents them

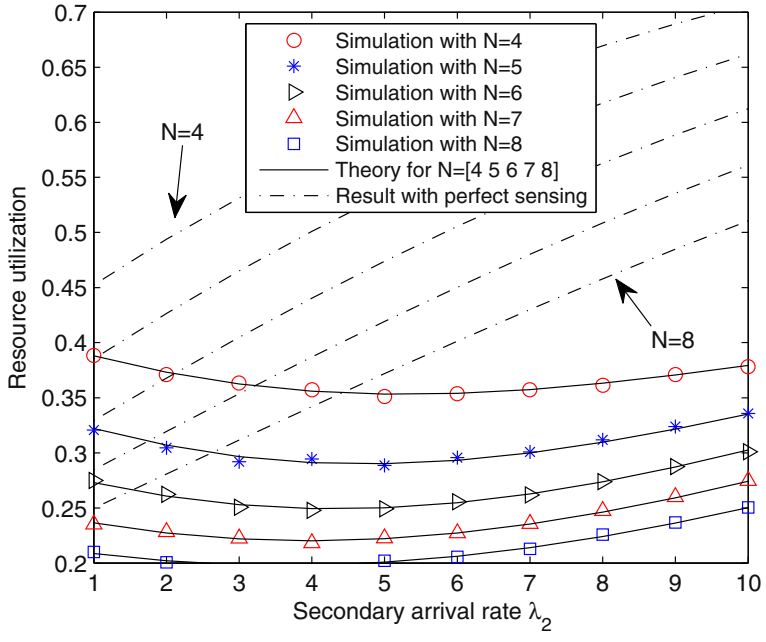

Fig. 12 System resource utilization, $\lambda_1 = 7, \mu_1 = \mu_2 = 4, \widehat{T_{TOL}} = 1$

from using network resources because of the increasing spectrum handoff initiation, which may lead to premature connection termination. With a small N, the system resources will be highly utilized since PUs and SUs will occupy most of the channels. However, when N is large, the radio resources are not fully utilized and therefore decreases the overall system resource utilization.

8 Conclusions

We studied the effect of the false alarm rates λ_{FARs} on the operation of CRNs. We developed a CTMC-based analytical model to evaluate the performance of CRNs under realistic network operating conditions. The proposed model not only includes sensing errors by incoming SUs but also takes into account the misdetection and false alarm probabilities by ongoing SUs. The modeling approach described here is capable of examining other performance evaluation parameters such as the effect of interference tolerance $\widehat{T_{\mathrm{TOL}}}$ among PUs and SUs as well as the effect of SU residual self-interference. We derived formulas for different performance metrics, including primary and secondary forced termination probabilities as well as secondary self-termination probability. Furthermore, we performed extensive simulations to validate the accuracy of the analytical model. Simulation results are in excellent agreement with the analytical results.

Results have shown that λ_{FAR} greatly influences the performance of CRNs by degrading SU performance and reducing network resource utilization. Results have also shown that decreasing the interference tolerance $\widehat{T_{\mathrm{TOL}}}$ has negative effect on the performance of PUs as it reduces primary successful probability and increases their forced termination probability. A similar effect was also observed with the increase in the SU residual interference distortion factor. Large amount of residual interference deteriorates the detection probability and leads to a reduced PU performance. The incorporation of λ_{FAR} into the CTMC model allows for obtaining exact and accurate state transition probabilities that improves calculation of the performance evaluation measures. The results of the proposed analytical model provide a new insight into the operation of CRNs and can be used to develop practical and more accurate CRN performance evaluation models. In future work, cooperative spectrum sensing can be considered for improving detection performance and/or for mitigating the effects of fading. Further study is also needed to investigate the case where on collisions, only SU calls will be terminated. Additionally, adaptive sensing parameters based on PU channel utilization can also be studied.

Competing interests

The authors declare that they have no competing interests.

Acknowledgements

The work of Janne Lehtomäki was supported by the Research Council of the University of Oulu. The work of Kenta Umebayashi was supported by the Strategic Information and Communications R&D Promotion Programme (SCOPE).

Author details

[1] Department of Communications Engineering (DCE), University of Oulu, Oulu 90014, Finland. [2] Centre for Wireless Communications (CWC), University of Oulu, Oulu 90014, Finland. [3] Department of Electrical and Electronic Engineering, Tokyo University of Agriculture and Technology, Tokyo, Japan.

Received: 10 May 2015 Accepted: 30 October 2015
Published online: 10 November 2015

References

1. J Mitola III. Cognitive radio: an integrated agent architecture for software defined radio. PhD thesis, Royal Institute of Technology, Sweden (2000)
2. S Haykin, Cognitive radio: brain-empowered wireless communications. IEEE J. Sel. Areas. Commun. **23**(2), 201–220 (2005)
3. IF Akyildiz, W-Y Lee, MC Vuran, S Mohanty, A survey on spectrum management in cognitive radio networks. IEEE Commun. Lett. **46**(4), 40–48 (2008)
4. A Ghasemi, ES Sousa, Spectrum sensing in cognitive radio networks: requirements, challenges and design trade-offs. IEEE Commun. Mag. **46**(4), 32–39 (2008)
5. L Luo, S Roy, Efficient spectrum sensing for cognitive radio networks via joint optimization of sensing threshold and durations. IEEE Trans. Commun. **60**(10), 2851–2860 (2012)
6. T Yucek, H Arslan, A survey of spectrum sensing algorithms for cognitive radio applications. IEEE Commun. Surv. Tutorials. **11**(1), 116–130 (2009)
7. J Lehtomäki. Analysis of energy based signal detection. PhD thesis, University of Oulu (2005). http://herkules.oulu.fi/isbn9514279255/isbn9514279255.pdf
8. JJ Lehtomäki, R Vuohtoniemi, K Umebayashi, On the measurement of duty cycle and channel occupancy rate. IEEE J. Sel. Areas Commun. **31**(11), 2555–2565 (2013)
9. H Urkowitz, Energy detection of unknown deterministic signals. Proc. IEEE. **55**(4), 523–531 (1967)
10. RA Dillard, GM Dillard, *Detectability of Spread-Spectrum Signals*. (Artech House, Norwood, 1989), p. 149
11. GM Dillard, M Reuter, J Zeiddler, B Zeidler, Cyclic code shift keying: a low probability of intercept communication technique. IEEE Trans. Aerosp. Electron. Syst. **39**(3), 786–798 (2003)
12. D-J Lee, M-S Jang, Optimal spectrum sensing time considering spectrum handoff due to false alarm in cognitive radio networks. IEEE Commun. Lett. **13**(2), 899–901 (2009)
13. RG Gallager, *Discrete Stochastic Processes*. (Kluwer Academic Publishers, Norwell, Massachusetts, 1996), p. 271
14. H Kim, KG Shin, Efficient discovery of spectrum opportunities with MAC-layer sensing in cognitive radio network. IEEE Trans. Mob. Comput. **7**(5), 533–545 (2008)
15. C Jiang, Y Chen, KJR Liu, Y Ren, Renewal-theoretical dynamic spectrum access in cognitive radio network with unknown primary behavior. IEEE J. Sel. Areas Commun. **31**(3), 406–416 (2013)
16. C Zhang, KG Shin, What should secondary users do upon incumbents' return? IEEE J. Sel. Areas Commun. **31**(3), 417–428 (2013)
17. C Jiang, Y Chen, Y Gao, KJR Liu, Joint spectrum sensing and access evolutionary game in cognitive radio networks. IEEE Trans. Wirel. Commun. **12**(5), 2470–2483 (2013)
18. J-l Wang, Y-h Xu, Z Gao, Q-h Wu, Discrete-time queuing analysis of opportunistic spectrum access: single user case. Frequenz. **65**(11–12), 335–341 (2011)
19. J Ko, H Ko, C Kim, Fast primary user detection during ongoing opportunistic transmission in OFDM-based cognitive radio. Wirel. Pers. Commun. **70**(4), 1463–1471 (2013)
20. E Ahmed, A Eltawil, A Sabharwal, in *proc. IEEE International Symposium on Antennas and Propagation Society (APSURSI)*. Simultaneous transmit and sense for cognitive radios using full-duplex: A first study (Chicago, USA, 2012), pp. 8–14

21. T Ihalainen, A Viholainen, TH Stitz, M Renfors, in *proc. IEEE International Conference on Cognitive Radio Oriented Wireless Networks and Communications (CROWNCOM)*. Reappearing primary user detection in cognitive radios (Cannes, France, 2010), pp. 1–5
22. W Lee, D-H Cho, in *proc. IEEE Wireless Communications and Networking Conference (WCNC)*. Concurrent spectrum sensing and data transmission scheme in a CR system (Las Vegas, USA, 2012), pp. 1326–1330
23. T Riihonen, S Werner, R Wichman, Mitigation of loopback self-interference in full-duplex MIMO relays. IEEE Trans. Sig. Process. **59**(12), 5983–5993 (2011)
24. K Umebayashi, JJ Lehtomäki, S Hatakeyama, Y Suzuki, in *proc. IEEE Personal Indoor and Mobile Radio Communications (PIMRC), Wireless distributed network workshop*. Cyclostationary spectrum sensing under four-level hypothesis for spectrum sharing (Toronto, Canada, 2011), pp. 2338-2343
25. W Han, J Li, Q Liu, L Zhao, Spatial false alarms in cognitive radio. IEEE Commun. Lett. **5**(5), 518–520 (2011)
26. S Tang, Y Xie, Performance analysis of unreliable sensing for an opportunistic spectrum sharing system. Int. J. of Commun. Netw. Inf. Secur. (IJCNIS). **3**(3), 240–246 (2011)
27. B Wang, Z Ji, KJR Liu, TC Clancy, Primary-prioritized Markov approach for dynamic spectrum allocation. IEEE Trans. Wirel. Commun. **8**(4), 1854–1865 (2009)
28. S Tang, BL Mark, Modeling and analysis of opportunistic spectrum sharing with unreliable spectrum sensing. IEEE Trans. Wirel. Commun. **8**(4), 1934–1943 (2009)
29. Y Zhang, in *proc. IEEE Int. Conf. Commun.* Dynamic spectrum access in cognitive radio wireless networks (Beijing, China, 2008), pp. 4927–4932
30. IM Suliman, JJ Lehtomäki, K Umebayashi, M Katz, Analysis of cognitive radio networks with imperfect sensing. IEICE Trans. Commun. **E96-B**(06), 1605–1615 (2013)
31. R Zhang, Y-C Liang, S Cui, Dynamic resource allocation in cognitive radio networks. IEEE Signal Process. Mag. **27**(3), 102–114 (2010)
32. R Urgaonkara, MJ Neely, Opportunistic scheduling with reliability guarantees in cognitive radio networks. IEEE Trans. Mob. Comput. **8**(6), 766–777 (2009)
33. M Höyhtyä. Adaptive power and frequency allocation strategies in cognitive radio systems. PhD thesis, University of Oulu 2014. http://www.vtt.fi/inf/pdf/science/2014/S61.pdf
34. BF Lo, A survey of common control channel design in cognitive radio networks. Phys. Commun. **4**(1), 26–39 (2011)
35. W Yin, P Ren, Q Du, Y Wang, Delay and throughput oriented continuous spectrum sensing schemes in cognitive radio networks. IEEE Trans. Wirel. Commun. **11**(6), 2148–2159 (2012)
36. S Hong, J Brand, JI Choi, M Jain, J Mehlman, S Katti, P Levis, Applications of self-interference cancellation in 5G and beyond. IEEE Commun. Mag. **52**(2), 114–121 (2014)
37. S Li, RD Murch, An investigation into baseband techniques for single-channel full-duplex wireless communication systems. IEEE Trans. Wirel. Commun. **13**(9), 4794–4806 (2014)
38. D Choi, D Park, Effective self interference cancellation in full duplex relay systems. Electron. Lett. **48**(2), 129–130 (2012)
39. JR Krier, IF Akyildiz, in *in proc. IEEE Personal Indoor and Mobile Radio Communications (PIMRC)*. Active self-interference cancellation of passband signals using gradient descent (London, UK, 2013), pp. 1212–1216
40. FF Digham, M-S Alouini, MK Simon, in *proc. IEEE International Conference on Communications (ICC)*. On the energy detection of unknown signals over fading channels (Alaska, USA, 2003), pp. 3575–3579
41. AH Nuttall, Some integrals involving the Qm function. IEEE Trans. Inf. Theory. **21**(1), 95–96 (1975)
42. T Riihonen, R Wichman, in *IEEE International Conference on Cognitive Radio Oriented Wireless Networks and Communications (CROWNCOM)*. Energy detection in full-duplex cognitive radios under residual self-interference (Oulu, Finland, 2014), pp. 57–60
43. L Yun, L Song, Z Han, Y Li, Full duplex cognitive radio: a new design paradigm for enhancing spectrum usage. IEEE Commun. Mag. **53**(5), 138–145 (2015)
44. W Afifi, M Krunz, Incorporating self-interference suppression for full-duplex operation in opportunistic spectrum access systems. IEEE Trans. Wirel. Commun. **14**(4), 2180–2191 (2015)
45. W Afifi, M Krunz, in *proc. IEEE International Symposium on Dynamic Spectrum Access Networks (DYSPAN)*. Adaptive transmission-reception-sensing strategy for cognitive radios with full-duplex capabilities (McLean, USA, 2014), pp. 149–160
46. W Afifi, M Krunz, in *proc. IEEE International Conference on Computer Communications (INFOCOM)*. Exploiting self-interference suppression for improved spectrum awareness/efficiency in cognitive radio systems (Turin, Italy, 2013), pp. 1258–1266
47. Y Xiao, I Ahmad, M Gao, J Yang, Y Zhang, Z Feng, Y Zhang, in *proc. IEEE Vehicular Technology Conference (VTC Fall)*. Improved energy detector for full duplex sensing (Vancouver, Canada, 2014), pp. 1-5
48. E Brookner, False alarm rate and false alarm number for discrete and continuous time sampling. IEEE Trans. Aerosp. Electron. Syst. **AES-17**(6), 809–814 (1981)
49. VG Kulkarni, *Modeling and Analysis of Stochastic Systems*. (CRC Press, London, 1995)
50. L Kleinrock, *Queueing Systems. Volume 1: Theory*, 1st edn. (Wiley-Interscience, New York, 1975), p. 417
51. G Ciardo, AS Miner, M Wan, AJ Yu, Approximating stationary measures of structured continuous-time Markov models using matrix diagrams. ACM SIGMETRICS Perform. Eval. Rev. **35**(3), 16–18 (2007)
52. P Buchholz, WH Sanders, in *proc. IEEE First International Conference on the Quantitative Evaluation of Systems (QEST 2004)*. Approximate computation of transient results for large Markov chains (Enschede, The Netherlands, 2004), pp. 126–135